4 Kinetic Energy Harvesting

4.1 Introduction

Kinetic energy harvesters convert energy from mechanical movements to electrical. A large number of applications can be classified under this category as there are many different types of mechanical movements such as vibrations, displacements, and forces or pressure and consequently different types of transducing mechanisms.

One may identify applications related to buildings and other construction projects such as bridges, exploring vibrations originating from a plurality of sources such as nearby or ongoing car automotive or train traffic; human movement; wind; heating; ventilating, and air conditioning (HVAC) air currents; and water and other fluid movements [63]. Vibration energy can be harvested in moving vehicles such as cars, trains, ships, and airplanes by properly installing transducers in sensitive places of the vehicle, such as the wheels of the car.

One may also distinguish between large-scale projects such as wind farms or hydroelectric energy plants and microenergy harvesting systems. Finally, one should mention kinetic energy harvesting applications involving human body movement [89], such as automatic watches harvesting energy from human arm movement and more recent applications harvesting energy from walking (or running) activities [10].

The chapter begins with a description of the three different transducing types associated with kinetic energy harvesting and then continues with a mathematical model and theoretical expressions for the maximum harvester energy and efficiency. A comparison of the performance of the the transducer types follows with a brief discussion of figures of merit. Finally, some selected examples of kinetic energy harvesters are provided.

4.2 Transducer Types

There are three transducing mechanisms that are used to convert kinetic energy to electrical energy: (a) electrostatic (capacitive), (b) electromagnetic (inductive), and (c) piezoelectric. The principle of operation and physics behind each mechanism is described in the following subsections.

https://doi.org/10.1017/9781139600255.005 Published online by Cambridge University Press

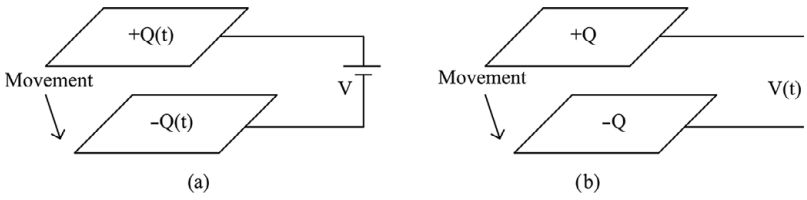

Figure 4.1 Electrostatic energy harvesting transducer: (a) fixed voltage and (b) fixed charge.

4.2.1 Electrostatic Transducers

Electrostatic transducers produce electrical energy by varying (a) the stored charge in a variable capacitor or (b) the voltage of a variable capacitor (Figure 4.1) [90]. The stored energy in a capacitor C is given by

$$E = \frac{1}{2}QV = \frac{1}{2}CV^2 = \frac{1}{2}\frac{Q^2}{C}, \tag{4.1}$$

where $Q = CV$ is the stored charge and V the voltage across its plates.

In the first method, in a first step, a variable capacitor is charged to a voltage V_{max} at a maximum capacitance C_{max}. In a second step, the capacitance is reduced to C_{min} employing, for example, mechanical movement of the capacitor plates, while the voltage across its plates is maintained at V_{max}. The produced energy by this procedure is

$$\Delta E = \frac{1}{2}\left(C_{max} - C_{min}\right)V_{max}^2. \tag{4.2}$$

The disadvantage of this method is that a voltage generator is required in order to maintain the voltage across the capacitor plates constant.

In the second method, the capacitor is first charged to a certain charge at the maximum capacitance, which creates a voltage $Q = C_{max}V_1$ across its terminals. The capacitance is then decreased to a value C_{min}, using for example mechanical means, while the capacitor terminals are kept as an open circuit in order to maintain its charge Q. As a result, the voltage across its plates is increased to $V_{max} = Q/C_{min}$ and electrical energy is produced:

$$\Delta E = \frac{1}{2}Q\left(V_{max} - V_{min}\right) = \frac{1}{2}\left(C_{max} - C_{min}\right)V_{max}V_1. \tag{4.3}$$

One can verify by comparing (4.2) and (4.3) that the amount of energy that is produced by the method of constant charge is less than the one produced by the architecture of constant voltage by a factor of V_{max}/V_1. However, the method of constant charge does not require any voltage generator circuitry, and consequently it is more easily implemented. Both architectures, however, require an initial charging phase of the capacitor before energy can be harvested. Nonetheless, a very attractive property of electrostatic transducers is that they can easily be integrated with other electronic circuitry, as microelectromechanical

https://doi.org/10.1017/9781139600255.005 Published online by Cambridge University Press

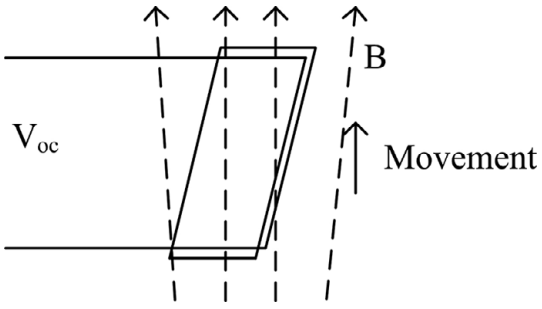

Figure 4.2 Electromagnetic energy harvesting transducer.

systems (MEMS) can be used to fabricate variable capacitor-based electrostatic transducers [63, 91].

4.2.2 Electromagnetic Transducers

Electromagnetic transducers are based on Faraday's law of induction. A schematic of such a transducer is shown in Figure 4.2. Specifically, an electromotive force, a voltage difference, is produced between the edges of a conductor when it moves inside a magnetic field. Typically, a coil is used as the conducting material and a permanent magnet generates the required magnetic field. Mechanical movement of the coil relative to the magnet results in a time-varying magnetic flux through the coil and subsequently an open-circuit voltage V_{oc}, which is equal to

$$V_{oc} = -N\frac{d\Phi}{dt}, \tag{4.4}$$

where N is the number of turns of the coil and Φ the magnetic field flux. Well-known examples are Faradays disc [92], a rotating coil inside a uniform static magnetic field, and Tesla's dynamo [93].

If one considers a coil that is moving along a path $x(t)$ inside a magnetic field B, (4.4) becomes

$$V_{oc} = -N\frac{d\Phi}{dx}\frac{dx}{dt} = D\frac{dx}{dt}. \tag{4.5}$$

In the case of a coil moving along the direction x with its area A oriented perpendicularly to a magnetic field with a magnitude gradient dB/dx, as shown in Figure 4.2, the open-circuit voltage becomes

$$V_{oc} = -NA\frac{dB}{dx}\frac{dx}{dt}. \tag{4.6}$$

An example of such a topology was used in [94], where the authors estimated that about 400 μW could be generated on average. Most of the rotating-type generators found today, from bicycle dynamos to large-scale power generation plants such as hydroelectric installations and wind farms, are electromagnetic transducers [94].

https://doi.org/10.1017/9781139600255.005 Published online by Cambridge University Press

4.2.3 Piezoelectric Transducers

The third type of mechanical to electric energy transducers is piezoelectric transducers. Piezoelectric materials produce an electric field when they are deformed. Conversely, when an electric field is applied to a piezoelectric material, it changes its form. The piezoelectric phenomenon is attributed to the presence of electric dipole moments within the material [63]. Application of pressure causes the microscopic dipole moments to align and results in a macroscopic polarization vector and a voltage difference along the material. The constitutive relations of a piezoelectric material are as follows [95, 96]:

$$\begin{aligned} \boldsymbol{S} &= \sigma \boldsymbol{T} + d^T \boldsymbol{E} \\ \boldsymbol{D} &= d\boldsymbol{T} + \epsilon \boldsymbol{E}, \end{aligned} \tag{4.7}$$

where $\boldsymbol{S}$ is the strain, $\boldsymbol{T}$ is the stress, $\boldsymbol{E}$ the electric field, and $\boldsymbol{D}$ the electric displacement. Bold type is used to indicate vector quantities. Furthermore, σ and ϵ are the compliance and permittivity tensors respectively. The piezoelectric strain is also a tensor quantity indicated by d. The superscript $()^T$ is used to indicate a matrix transpose. In absence of piezoelectric strain, the second equation becomes the standard constitutive equation between displacement $\boldsymbol{D}$ and electric field $\boldsymbol{E}$.

Piezoelectric materials are anisotropic materials, and as such they have a different behavior depending on the direction of the stress $\boldsymbol{T}$ and the electric field $\boldsymbol{E}$. Specifications of piezoelectric materials typically provide a piezoelectric strain constant d using two subscript indices, the first one referring to the direction of the electric field and the second to the direction of the stress. The three axes x, y and z are indicated using the indices 1, 2, and 3 respectively. As an example, a piezoelectric strain constant d_{33} refers to a piezoelectric system topology where both the electric field and the stress are applied along the z-direction that corresponds to the thickness of the piezoelectric material, as shown in Figure 4.3 [63]. Commonly used piezoelectric materials are ferroelectric perovskites and piezoelectric polymer materials [63, 96]. A characteristic representative of perovskite ceramic materials is lead zirconatetitanate $Pb(Zr,Ti)O_3$, (PZT), whereas a commonly used piezoelectric polymer is polyvinylidene fluoride (PVDF).

4.3 Modeling Vibration Energy Harvesting Systems

Williams and Yates have proposed a model for electric generators harvesting energy from a mechanical vibration motion that is widely used [97]. The model consists of a mass m that is attached to a spring of stiffness k from a frame that is excited by an external source y as shown in Figure 4.4. As a result of the external excitation y, the mass m is displaced relative to the frame by z. Losses in the transfer of kinetic energy from the external source y to the mass m are indicated by the damping coefficient $d_T = d_m + d_e$, which includes

https://doi.org/10.1017/9781139600255.005 Published online by Cambridge University Press

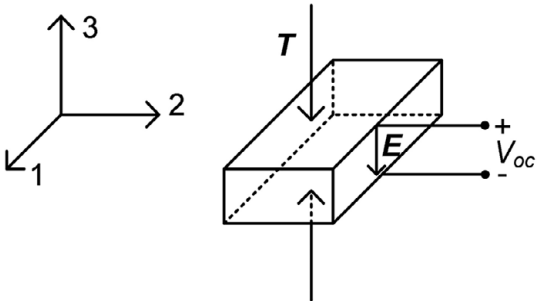

Figure 4.3 Piezoelectric strain constant d_{33} example system.

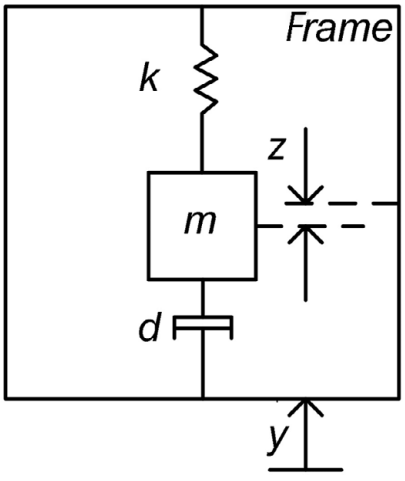

Figure 4.4 Model of a electric energy generator based on kinetic energy harvesting [97].

both mechanical parasitic losses d_m as well as losses d_e corresponding to energy conversion from mechanical to electrical. The system dynamics are described by the second-order differential equation

$$m\ddot{z} + d_T\dot{z} + kz = -m\ddot{y}. \tag{4.8}$$

The system differential equation can be expressed in a normalized form

$$\ddot{z} + 2\zeta_T\omega_n\dot{z} + \omega_n^2 z = -\ddot{y}, \tag{4.9}$$

where ω_n is the natural frequency of oscillation of the system and

$$\zeta_T = \frac{d}{2m\omega_n} \tag{4.10}$$

is the damping factor, which comprises two contributions, ζ_m corresponding to parasitic mechanical losses d_m and ζ_e corresponding to the mechanical-to-electrical conversion losses d_e. One obtains the steady-state response of the system by taking the Fourier transform of (4.8) or (4.9),

https://doi.org/10.1017/9781139600255.005 Published online by Cambridge University Press

$$Z(\omega) = \frac{\left(\frac{\omega}{\omega_n}\right)^2}{1 - \left(\frac{\omega}{\omega_n}\right)^2 + j2\zeta_T\left(\frac{\omega}{\omega_n}\right)} Y(\omega) = A(\omega)Y(\omega). \tag{4.11}$$

Assuming a sinusoidal excitation $y(t) = Y_o \sin(\omega t)$ and taking the inverse Fourier transform of (4.11), one obtains the time domain displacement $z(t)$ of the mass m as

$$z(t) = \frac{\left(\frac{\omega}{\omega_n}\right)^2 Y_o}{\sqrt{\left[1 - \left(\frac{\omega}{\omega_n}\right)^2\right]^2 + \left(2\zeta_T \frac{\omega}{\omega_n}\right)^2}} \sin(\omega t + \phi) \tag{4.12}$$

with

$$\phi = -\tan^{-1}\left(\frac{2\zeta_T \frac{\omega}{\omega_n}}{1 - \left(\frac{\omega}{\omega_n}\right)^2}\right). \tag{4.13}$$

The instantaneous electrical power P_e that is generated is the power dissipated due to d_e, which is equal to the force $F_e = d_e\dot{z} = 2\zeta_e m\omega_n \dot{z}$ corresponding to the damping coefficient d_e, multiplied by the velocity $\dot{z}$, i.e., $P_e = F_e\dot{z}$. The average generated electrical power is therefore given by

$$P_e = d_e < \dot{z}^2 > = \ 2\zeta_e m\omega_n < \dot{z}^2 >, \tag{4.14}$$

where <> denotes a time average. Taking the time derivative of the steady-state solution (4.12) in order to find $\dot{z}$ and applying it in the expression for the average generated power (4.14), one calculates the average electrical power generated as

$$P_e = \frac{\zeta_e m\omega_n \left(\frac{\omega}{\omega_n}\right)^4 \omega^2 Y_o^2}{\left[1 - \left(\frac{\omega}{\omega_n}\right)^2\right]^2 + \left(2\zeta_T \frac{\omega}{\omega_n}\right)^2} = \frac{\zeta_e m \left(\frac{A^2\omega^2}{\omega_n^3}\right)}{\left[1 - \left(\frac{\omega}{\omega_n}\right)^2\right]^2 + \left(2\zeta_T \frac{\omega}{\omega_n}\right)^2}, \tag{4.15}$$

where $A = \omega^2 Y_o$ is the acceleration of the external excitation y. Maximum power conversion occurs when the excitation y has the same frequency as the natural frequency of the system $\omega = \omega_n$, resulting in

$$P_{em} = \frac{m\zeta_e \omega_n^3 Y_o^2}{4\zeta_T^2} = \frac{m\zeta_e A^2}{4\zeta_T^2 \omega_n}. \tag{4.16}$$

The generated power is strongly dependent on how close the excitation frequency ω is to the system natural frequency ω_n. This is visualized next by expressing the average generated power relative to its maximum value as

$$\frac{P_e}{P_{em}} = \frac{4\zeta_T^2 \left(\frac{\omega}{\omega_n}\right)^2}{\left[1 - \left(\frac{\omega}{\omega_n}\right)^2\right]^2 + 4\zeta_T^2 \left(\frac{\omega}{\omega_n}\right)^2}. \tag{4.17}$$

https://doi.org/10.1017/9781139600255.005 Published online by Cambridge University Press

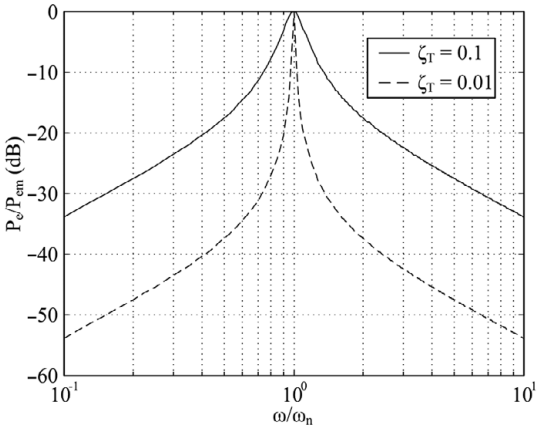

Figure 4.5 Dependence of the generated power on frequency for different damping coefficients.

The variation of the generated power with respect to the frequency of the external excitation relative to the resonance frequency of the system is shown in Figure 4.5 for $\zeta_T = 0.1$ and $\zeta_T = 0.01$.

The strong dependence on the natural resonance frequency of the system is one of the main drawbacks of vibration to electric transducers as it makes their design very application dependent. One should first accurately determine by simulation or measurement the frequency of excitation corresponding to the specific application scenario and subsequently design a generator with the same natural frequency of oscillation. A great challenge in the vibration to electrical transducer design is that of maximizing harvested energy by controlling the natural frequency of the transducers. There are several different possibilities proposed in the literature that include transducers with mechanically or electrically tunable resonant frequencies and self-tuning or adaptive tuning capability on one hand, and wideband and multiband arrays of generators on the other hand [63, 98].

One may further maximize P_e by taking its derivative versus the damping factor ζ_e and setting it equal to zero in order to solve for the optimum damping factor $\zeta_e = \zeta_{em}$. A straightforward calculation gives that the optimum value of the damping factor ζ_{em} is equal to half the total damping factor ζ_T or, in other words, when the electrical and parasitic mechanical damping factors are equal, $\zeta_{em} = \zeta_m = \zeta_T/2$, which gives

$$P_{emo} = \frac{m\omega^3 Y_o^2}{16\zeta_{em}} = \frac{mA^2}{16\zeta_{em}\omega_n}. \tag{4.18}$$

Therefore, the maximum generated power is proportional to the square of the external signal acceleration amplitude A, proportional to the mass m of the system and inversely proportional to the natural resonance frequency ω_n of the system and the damping factor ζ_{em}. In general, in order to maximize the electrical

https://doi.org/10.1017/9781139600255.005 Published online by Cambridge University Press

output power of the system, the mass of the system should be maximized and the system should be operated in its lower resonance frequency [99].

Finally, one should emphasize the generality of the model by Williams and Yates, which can be used to model any kind of vibration to electric energy transducer, electrostatic, electromagnetic, or piezoelectric. One limitation of the model is that the conversion to electric energy is taken into account by considering a linear term in the system differential equation through a damping coefficient, which may not always be accurate [91]. One of the most important tasks of the designer becomes that of computing and optimizing the value of the damping factor for the system under consideration, which is typically evaluated using numerical techniques such as a finite element method simulator [63].

4.4 Vibration Sources

The theoretical analysis has shown that the maximum generated electrical power depends on the acceleration A and the frequency $\omega_n = 2\pi f_n$ of the external vibration sources. A fundamental task of the designer of a kinetic energy harvesting system is to determine these parameters for the application under consideration. Such an analysis was carried out in [100], where several external vibration source scenarios were studied and the acceleration and vibration frequencies were evaluated. Table 4.1 includes a selection of the results published in [100]. One can see that the source frequencies are in the order of a few tens to a few 100 Hz, whereas the acceleration values range from 0.1 ms^{-2} to 3 ms^{-2}.

Table 4.1 Measured frequencies and acceleration amplitude of various vibration sources [100].

Application, vibration source	Vibration frequency (Hz)	Acceleration amplitude (ms^{-2})
Door frame just as door closes	125	3
Clothes dryer	121	3.5
Washing machine	109	0.5
HVAC vents in office building	60	0.2–1.5
Refrigerator	240	0.1
Small microwave oven	121	2.25
External windows (2 ft × 3 ft) next to a busy street	100	0.7

https://doi.org/10.1017/9781139600255.005 Published online by Cambridge University Press

4.5 Comparison of Different Kinetic Energy Harvesters

An immediate question that comes to mind is how do the different types of vibration harvesters compare with each other. In order to address this question, a linear, two-port model for a general kinetic energy transducer was considered in [100]. The performance of the transducer is determined by two parameters, the coupling coefficient κ and the transmission coefficient λ. The transmission coefficient λ is equal to the efficiency of the transducer, the ratio of the energy delivered to the load to the average input energy to the transducer. The coupling coefficient κ instead is equal to the energy stored within the transducer over the average input energy. The maximum transmission coefficient λ_m was found to be equal to [100]

$$\lambda_m = \frac{\kappa^2}{4 - 2\kappa^2}. \tag{4.19}$$

Assuming a harmonic external excitation with frequency ω and input energy U_i, the maximum power delivered to the load is

$$P_m = \lambda_m \omega U_i. \tag{4.20}$$

The coupling coefficient κ was computed for different types of kinetic energy transducers in [100], which allows one to compare the different transducers. Specifically, the coupling factor of an electromagnetic generator was evaluated to be

$$\kappa_{em}^2 = \frac{(Bl)^2}{k_{sp}L}, \tag{4.21}$$

where B is the magnetic flux density, k_{sp} the spring inductance, l is the length of the wire in the coil, and L the coil inductance. In the case of piezoelectric generators, the coupling factor was evaluated as

$$\kappa_{em}^2 = \frac{dE}{\epsilon}, \tag{4.22}$$

where d is the piezoelectric strain coefficient, E is Young's modulus, and ϵ the dielectric permittivity. Electrostatic transducers are nonlinear, and consequently the coupling coefficient depends on the amplitude of the input excitation. Based on the preceding analysis, it was determined in [100] that comparable efficiencies and maximum generated power can be obtained for electromagnetic and piezoelectric devices. In the case of electrostatic devices, the comparison is more difficult due to the nonlinear nature of the devices, but it was also determined that for a given input excitation amplitude, comparable coupling coefficients may also be obtained.

https://doi.org/10.1017/9781139600255.005 Published online by Cambridge University Press

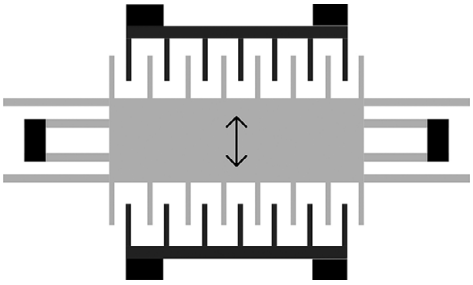

Figure 4.6 MEMS-based electrostatic energy harvester layout representation, based on [90].

4.6 Vibration Energy Harvester Examples

There are many kinetic energy harvesting device examples in the literature, as the fundamental physics behind the kinetic-to-electrical energy conversion has been studied for many years. As an example, it has been already noted in Section 4.2.2 that Tesla's electromagnetic dynamo transducer was patented in 1887 [93]. Technology, however, is making possible new implementations especially tailored toward microenergy scavenging or harvesting applications.

Silicon micromachining MEMS technology is particularly suitable for implementing mechanically tunable capacitors for electrostatic transducers due to its compatibility for integration with silicon microelectronics and its availability for mass production [91]. The first MEMS-based electrostatic microenergy generator in the literature was reported in [90]. The simulated harvested energy by the transducer was 8.6 μW, whereas approximately 5.6 μW would be usable and the rest would be dissipated by the controller. A view of the capacitor layout is shown in Figure 4.6. The capacitor comprises two anchored stationary comb terminals and an oscillating mass in the middle. This topology is known as in-plane overlap type, where the capacitance changes by varying the overlapping between the fingers. There exist two additional topologies, the in-plane gap closing, a conceptual view of which is shown in Figure 4.7, and the out-of-plane gap closing shown in Figure 4.8 [91, 99].

A characteristic example of a piezoelectric-based vibration energy harvester is the one developed by Roundy and Wright [101]. The structure comprises a piezoelectric bimorph with an attached mass M, shown in Figure 4.9. A bimorph is a cantilever that comprises two sheets of piezoelectric material sandwiched together with a center nonpiezoelectric shim and bonded together. As the cantilever bends, one of the piezoelectric sheets is stretched and the other is compressed according to the direction of the bending force. The bimorph is operated in the 31 mode, exploring the strain d_{31} tensor element where the stress is applied in the z direction and the electric field is generated along the x direction, as explained in Section 4.2.3. A prototype harvester was fabricated

https://doi.org/10.1017/9781139600255.005 Published online by Cambridge University Press

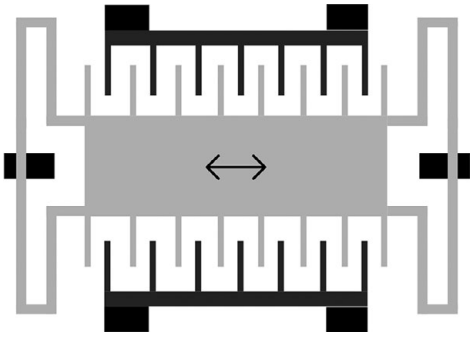

Figure 4.7 In-plane gap closing layout representation, based on [91, 99].

Figure 4.8 Out-of-plane gap closing layout representation, based on [91, 99].

where the bimorph was made with PZT-5A sheets sandwiched together with a steel shim and the mass was made from an alloy of tin and bismuth [101]. The structure was designed to resonate at 120 Hz and was tested with external vibrations with acceleration of 2.5 ms^{-2}. The prototype delivered about 80 μW at a 250 KΩ load. Subsequent further optimized designs were able to deliver up to 375 μW under the same excitation of 2.5 ms^{-2} at 120 Hz.

Shenk and Paradiso [10] demonstrated a body-worn piezoelectric energy harvester placed in the insole of a shoe. The concept is shown in Figure 4.10, which illustrates two possible topologies for the harvester, a semiflexible PZT-based bimorph placed under the heel or a flexible PVDF bimorph placed under the ball of the foot. The PVDF stave was able to harvest 1.3 mW on average in a 250 KΩ load at a 0.9 Hz walking pace. The PZT dimorph produced on average 8.4 mW in a 500 KΩ load under approximately the same walking pace. The harvester was used to power an active RFID tag operating at 310 MHz. Subsequently, Orecchini et al. demonstrated an RFID tag powered by a shoe-mounted piezoelectric energy

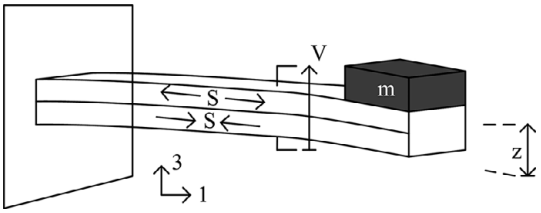

Figure 4.9 Piezoelectric bimorph energy harvester, based on [101].

https://doi.org/10.1017/9781139600255.005 Published online by Cambridge University Press

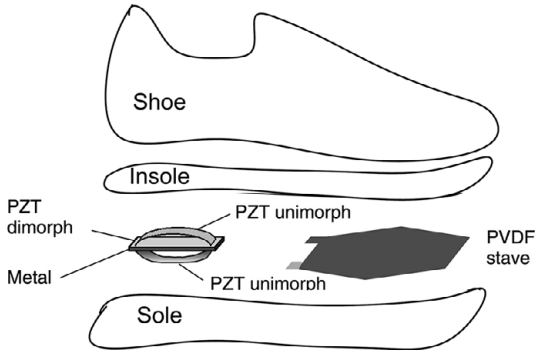

Figure 4.10 Schematic representation of a piezoelectric bimorph shoe-mounted energy harvester based on [10].

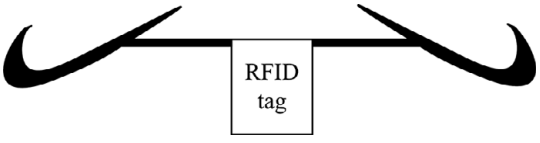

Figure 4.11 Schematic representation of shoe-mounted inkjet-printed RFID tag based on [102].

harvester where the electronic circuitry and the antenna were inkjet printed on a flexible paper substrate (see Figure 4.11) [102].

The world's first watch powered by an electromagnetic type vibration energy harvester was introduced in 1988 by Seiko [103]. The movement of the arm on which the watch is worn caused a rotor to rotate and subsequently spin an electromagnetic vibration–based harvester. The harvester is capable of powering the watch, which required only 0.7 μW.

An example of a miniature silicon-based electromagnetic-type vibration harvester is the one developed by Beeby et al. [104]. The device comprised four magnets and a coil implemented in a vibrating silicon cantilever paddle layer. The harvester was able to generate 21 nW from an external source with acceleration of 1.92 ms^{-}2 at 9.5 KHz [99].

Finally, a hybrid system combining an electromagnetic-type vibration energy harvester with a radio frequency (RF) energy harvester was introduced by Gu et al. [105]. A schematic of the circuit is shown in Figure 4.12. The output of an antenna is connected to a shunt diode rectifier circuit harvesting RF power and converting it to dc electrical power. The output of an electromagnetic-type vibration harvester comprising a coil placed inside the magnetic field of a permanent magnet is electrically connected in parallel to the shunt diode, which also rectifies it to produce a combined dc output current delivered to a load. The cooperating functionality of the two harvesters results in improved efficiency for the combined system. The implementation of hybrid harvesting systems provides an added challenge to the designer as the electrical connection

https://doi.org/10.1017/9781139600255.005 Published online by Cambridge University Press

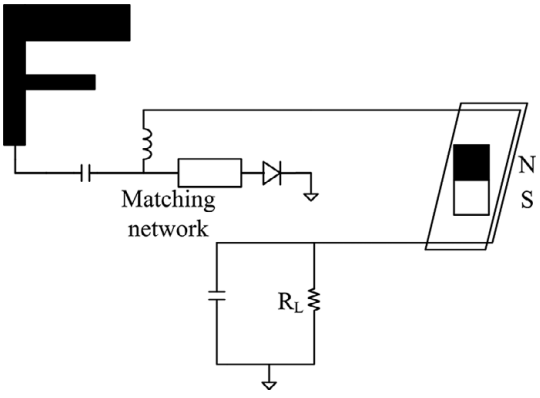

Figure 4.12 Schematic representation of hybrid vibration and an RF energy harvester based on [105].

of the two individual harvesters results in loading each other and consequently affecting their operating efficiency.

4.7 Problems and Questions

1. How many types of electrostatic transducers exist and what is their principle of operation?
2. What is the operating principle of electromagnetic transducers?
3. What is the operating principle of piezoelectric transducers? Name a ceramic and a polymer piezoelectric material. What does a piezoelectric strain constant d_{31} refer to?
4. Describe the model of vibration energy harvesting transducers proposed by Williams and Yates.
5. Order the various vibration sources listed in Table 4.1 according to the maximum available energy for harvesting assuming that the same harvesting transducer is installed on all of the sources.
6. If the available energy for harvesting by a constant voltage electrostatic energy harvester is 5 μW, how much is the required capacitance variation when the harvester capacitor is charged to 10 V?
7. What is the available energy for harvesting by a constant charge electrostatic energy harvester if the same capacitance variation is used as in the previous problem and the capacitor is first charged to a voltage of 5 V at a minimum capacitance and the maximum voltage across its plates is 10 V when the maximum capacitance is reached?
8. An electromagnetic transducer comprises a square coil with N = 20 turns and has a side with length 10 cm. The coil is allowed to vibrate along its axis x inside a magnetic field B that is also directed along axis x. The magnetic

https://doi.org/10.1017/9781139600255.005 Published online by Cambridge University Press

field has a slope of $dB/dx = 0.1$ T at the location of the coil. The vibration source makes the coil vibrate with an acceleration magnitude of 10 m/s^2 at a frequency of 2 Hz. What is the maximum open-circuit voltage magnitude at the coil terminals?

https://doi.org/10.1017/9781139600255.005 Published online by Cambridge University Press